

THE KONTSEVICH TETRAHEDRAL FLOWS REVISITED

A. BOUISAGHOUANE, R. BURING, AND A. KISELEV*

ABSTRACT. We prove that the Kontsevich tetrahedral flow $\dot{\mathcal{P}} = \mathcal{Q}_{a:b}(\mathcal{P})$, the right-hand side of which is a linear combination of two differential monomials of degree four in a bi-vector \mathcal{P} on an affine real Poisson manifold N^n , does infinitesimally preserve the space of Poisson bi-vectors on N^n if and only if the two monomials in $\mathcal{Q}_{a:b}(\mathcal{P})$ are balanced by the ratio $a : b = 1 : 6$.

Summary. The right-hand side $\mathcal{Q}_{a:b}$ of the Kontsevich tetrahedral flow $\dot{\mathcal{P}} = \mathcal{Q}_{a:b}(\mathcal{P})$ on the space of bi-vectors on an affine Poisson manifold (N^n, \mathcal{P}) is a linear combination of two differential monomials of degree four in the bi-vector \mathcal{P} that evolves. Recent counterexamples show that the bi-vector $\mathcal{P}|_{\varepsilon=0} + \varepsilon \mathcal{Q}_{a:b}(\mathcal{P}|_{\varepsilon=0}) + \bar{o}(\varepsilon)$ stays infinitesimally Poisson, that is, $[\mathcal{P}|_{\varepsilon=0}, \mathcal{Q}_{a:b}(\mathcal{P}|_{\varepsilon=0})] \doteq 0$ by virtue of the property $[\mathcal{P}|_{\varepsilon=0}, \mathcal{P}|_{\varepsilon=0}] = 0$ of the Cauchy datum to be Poisson, only if the balance $a : b$ in $\mathcal{Q}_{a:b}$ is equal to $1 : 6$. (Without extra assumptions, the infinitesimal deformation $\mathcal{P}|_{\varepsilon=0} + \varepsilon \mathcal{Q}_{a:b}(\mathcal{P}|_{\varepsilon=0}) + \bar{o}(\varepsilon)$ can be completed to a finite deformation $\mathcal{P}(\varepsilon)$ at $\varepsilon > 0$ only if the third Poisson cohomology group $H_{\mathcal{P}}^3(N^n)$ with respect to the differential $\partial_{\mathcal{P}} = [\mathcal{P}, \cdot]$ vanishes for the Poisson manifold (N^n, \mathcal{P}) . Therefore, unlike the Kontsevich formula for the flow $\dot{\mathcal{P}} = \mathcal{Q}_{a:b}(\mathcal{P})$ which is universal for all N^n and \mathcal{P} , the integration issue is Poisson model-dependent.)

We now prove that the balance $a : b = 1 : 6$ in the Kontsevich tetrahedral flow is universal in the above sense: for all Poisson bi-vectors \mathcal{P} on every affine manifold N^n , the deformation $\mathcal{P} + \varepsilon \mathcal{Q}_{1:6}(\mathcal{P}) + \bar{o}(\varepsilon)$ is infinitesimally Poisson. The proof is explicit. First the differential consequences of the identity $\text{Jac}(\mathcal{P}) := [\mathcal{P}, \mathcal{P}] = 0$ for Poisson bi-vectors are filtered up to order three according to the differential orders (k, ℓ, m) , $k + \ell + m \geq 3$, with respect to the arguments of the tri-vector $[\mathcal{P}, \mathcal{P}]$. To describe the differential operators that produce such consequences of the Jacobi identity, we use the pictorial language of graphs: every internal vertex contains a copy of the bi-vector \mathcal{P} and the operators are reduced by using its skew-symmetry. We recall that every differential consequence of order (k, ℓ, m) for the Jacobi identity $\text{Jac}(\mathcal{P}) = 0$ then vanishes. By implementing the Kontsevich graph calculus in software and running it on a (super)computer, we find the (non)linear polydifferential operator $\diamond(\mathcal{P}, \cdot)$ that acts on the filtered components of the Jacobiator $\text{Jac}(\mathcal{P})$ for the bi-vector \mathcal{P} and that reveals the factorization, $[\mathcal{P}, \mathcal{Q}_{1:6}(\mathcal{P})] = \diamond(\mathcal{P}, \text{Jac}(\mathcal{P}))$, of the $\partial_{\mathcal{P}}$ -cocycle condition for the flow $\dot{\mathcal{P}} = \mathcal{Q}_{1:6}(\mathcal{P})$ through the Jacobi identity $\text{Jac}(\mathcal{P}) = 0$.

Date: 4 August 2016.

2010 Mathematics Subject Classification. 53D55, 58E30, 81S10; secondary 53D17, 58Z05, 70S20.

Key words and phrases. Poisson bracket, affine manifold, graph complex, tetrahedral flow, Poisson cohomology.

Address: Johann Bernoulli Institute for Mathematics and Computer Science, University of Groningen, P.O. Box 407, 9700 AK Groningen, The Netherlands. **E-mail:* A.V.Kiselev@rug.nl.

Introduction. The main question which we address in this paper is how Poisson structures can be deformed in such a way that they stay Poisson. We reveal one such method that works for all Poisson structures on affine real manifolds; the construction of that flow on the space of bi-vectors was proposed in [12]: the formula is derived from two differently oriented tetrahedral graphs over four vertices. The flow is a linear combination of two terms, each quartic-nonlinear in the Poisson structure. By using several examples of Poisson brackets with high polynomial degree coefficients, we demonstrated in [1] that the ratio $1 : 6$ is the only possible balance at which the tetrahedral flow can preserve the property of the Cauchy datum to be Poisson. But does the Kontsevich tetrahedral flow $\hat{\mathcal{P}} = \mathcal{Q}_{1:6}(\mathcal{P})$ with ratio $1 : 6$ actually preserve the space of *all* Poisson bi-vectors? In dimension 3 the description of Poisson brackets with smooth coefficients is known from [4]; a brute force calculation then verifies the claim. In this paper, we prove the claim in full generality, namely, for all Poisson structures on all affine manifolds of arbitrary finite dimension. As a first by-product, our proof shows that there is no mechanism (that would involve the language of Kontsevich graphs) for the tetrahedral flow to be trivial in the respective Poisson cohomology. Secondly, the factorization mechanism, which is the core idea of the proof of Theorem 3, explains in hindsight why the proven property of the tetrahedral flows is false for the variational Poisson brackets. (This was observed empirically in [1]; the geometry of Poisson structures over jet bundles is known from [16].)

The text is structured as follows. In section 1 we recall how oriented graphs can be used to encode differential operators acting on the space of multivectors. In particular, differential polynomials in a given Poisson structure are obtained in the frames of this approach as soon as a copy of that Poisson bi-vector is placed in every internal vertex of a graph. Now that the calculus of multivectors is possible by using pictures, we engage the standard cohomological techniques to rephrase the main claim under study as the cocycle condition,

$$[\mathcal{P}, \mathcal{Q}_{1:6}(\mathcal{P})] \doteq 0 \quad \text{mod } [\mathcal{P}, \mathcal{P}] = 0, \quad (1)$$

with respect to the Poisson differential $\partial_{\mathcal{P}} = [\mathcal{P}, \cdot]$. (Here we denote by $[\cdot, \cdot]$ the Schouten bracket.) Section 1 concludes with our main theorem (namely, Theorem 3 on p. 6) which establishes the mechanism of (1). Section 2 contains the proof of Theorem 3. On the one side of the factorization problem (1) we expand the Poisson differential of the Kontsevich tetrahedral flow at the balance $1 : 6$ into the sum of 39 graphs. On the other side of that factorization, we take the sum that runs over all those fragments of differential consequences of the Jacobi identity $[\mathcal{P}, \mathcal{P}] = 0$ which are known to vanish independently, with undetermined coefficients. If a given such differential consequence contains one or several derivations falling on the internal vertices of the Jacobiator for the Poisson bi-vector \mathcal{P} , their action is expanded via the Leibniz rule(s). The resulting sum of graphs is reduced modulo the skew-symmetry of the bi-vector at hand; there remain 7,025 graphs, the coefficients of which are linear in the unknowns. We now solve the arising inhomogeneous linear algebraic system. Its solution yields the poly-differential operator \diamond , encoded using graphs (see p. 8) that provides the sought-for factorization $[\mathcal{P}, \mathcal{Q}_{1:6}] = \diamond(\mathcal{P}, \text{Jac}(\mathcal{P}))$. This completes the proof (the maximally detailed description of that solution is contained in Appendix C). Meanwhile, in section 3

we analyze the properties of the solution at hand. The paper concludes with a list of open problems.

In Appendix D we outline a different method to tackle the factorization problem, namely, by making the Jacobi identity visible in (1) by perturbing the original structure \mathcal{P} so that it stops being Poisson. Hence it contributes to the right-hand side of (1) such that the respectively perturbed bi-vector $\mathcal{Q}_{1:6}(\mathcal{P})$ stops being compatible with the perturbed Poisson structure. The first-order balance of both sides of perturbed equation (1) then suggests the coefficients of those differential consequences of the Jacobiator which are actually involved in the factorization mechanism. The coefficients of operators realized by graphs which were found by following this scheme were later reproduced in the full run-through that gave us the solution in section 2.

1. THE MAIN PROBLEM: FROM GRAPHS TO MULTIVECTORS

1.1. The language of graphs. Let us formalise a way to encode polydifferential operators – in particular multivectors – using oriented graphs. In an affine real manifold N^n (here $3 \leq n < \infty$), consider a chart $U_\alpha \hookrightarrow \mathbb{R}^n$ and denote the Cartesian coordinates by $\mathbf{x} = (x^1, \dots, x^n)$. By definition, the decorated edge $\bullet \xrightarrow{i} \bullet$ denotes at once the derivation $\partial/\partial x^i \equiv \partial_i$ (that acts on the content of the arrowhead vertex) and the summation $\sum_{i=1}^n$ (over the index i in the object which is contained within the arrowtail vertex). As it has been explained in [13, 6, 8] the operator which every graph encodes is equal to the sum (running over all the indexes) of products (running over all the vertices) of those vertices content (differentiated by the in-coming arrows, if any). For example, the graph $(1) \xleftarrow[L]{i} \mathcal{P}^{ij}(\mathbf{x}) \xrightarrow[R]{j} (2)$ encodes the bi-differential operator $\sum_{i,j=1}^n (1) \xleftarrow{i} \partial_i \cdot \mathcal{P}^{ij}(\mathbf{x}) \cdot \xrightarrow{j} (2)$. It then specifies the Poisson bracket on a chart $U_\alpha \subset N^n$. The bracket satisfies the Jacobi identity

$$\boxed{\bullet \bullet} = \begin{array}{c} \diagdown \quad \diagup \\ 1 \quad 2 \end{array} + \begin{array}{c} \diagup \quad \diagdown \\ 2 \quad 3 \end{array} + \begin{array}{c} \diagup \quad \diagdown \\ 3 \quad 1 \end{array} + \begin{array}{c} \diagdown \quad \diagup \\ 3 \quad 2 \end{array} = 0. \quad (2)$$

Clearly, the Jacobiator $\text{Jac}(\mathcal{P})$ is totally skew-symmetric with respect to its arguments 1, 2, 3.

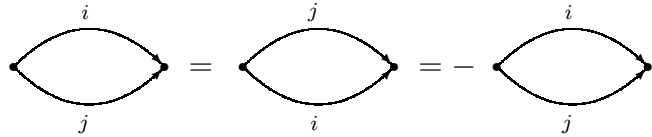
From now on, let us consider only the oriented graphs whose vertices are either sinks (with no issued edges) like the vertices 1, 2, 3 in (2) or tails for an ordered pair of arrows, each decorated with own index. (We refer to Jacobi identity (2), Figure 2 on p. 5, and to the graphical formulae on pp. 13, 8, 9). By definition, the arrowtail vertices are called *internal*; in particular, every source vertex, to which no arrows come, is an internal vertex of a graph. For each internal vertex \bullet , the pair of out-going edges is ordered L \prec R. Next, every internal vertex \bullet carries a copy of a given Poisson bi-vector $\mathcal{P} = \mathcal{P}^{ij}(\mathbf{x}) \partial_i \wedge \partial_j$ with its own pair of indices. The ordering L \prec R of decorated out-going edges coincides with the ordering “first \prec second” of the indexes in the coefficients of \mathcal{P} . Namely, the left edge (L) carries the first index and the other edge (R) carries the second index.

Remark 1. In principle, we allow the presence of both the tadpoles and cycles over two vertices (or “eyes”); see Figure 1. However, in hindsight there will be neither tadpoles nor eyes in the solution which we shall have found in section 2 below.

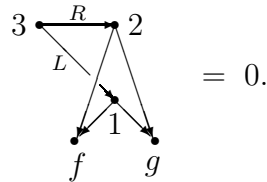


FIGURE 1. A tadpole and an “eye”.

Remark 2. Under the above assumptions, there exist inhabited graphs that encode zero differential operators. Namely, consider the graph with a double edge:



By first relabelling the summation indices and then swapping $L \leftrightarrows R$ we evaluate the operator acting at z to $\sum_{i,j=1}^n a^{ij} \partial_i \partial_j(z) = - \sum_{i,j=1}^n a^{ij} \partial_i \partial_j(z)$; whence the operator is zero. In the same way, any graph containing a double edge encodes a zero operator. Graphs can also encode zero differential operators in a more subtle way. For example consider the wedge on two wedges:



Swapping the labels of the lower wedges does not change the operator. On the other hand, swapping left and right in the top wedge introduces a minus sign. Hence the graph encodes a differential operator equal to minus itself, i.e. zero.

Besides the trivial vanishing mechanism in Remark 2, there is Jacobi identity (2) together with its differential consequences, which will play a key role in what follows.

1.2. The Kontsevich tetrahedral flow. In the paper [12], Kontsevich proposed the construction of flows $\dot{\mathcal{P}} = \mathcal{Q}(\mathcal{P})$ on the spaces of Poisson structures on affine real manifolds. In particular, he associated one such flow on the space of Poisson bi-vectors \mathcal{P} with the full graph over four vertices, that is, the tetrahedron. Up to symmetry, there are two essentially different ways, resulting in Γ_1 and Γ_2 , to orient its edges, provided that every vertex is a source for two arrows and, as an elementary count suggests, there are two arrows leaving the tetrahedron that act on the arguments of the bi-differential operator which the tetrahedral graph encodes. The two oriented tetrahedral graphs are shown in Fig. 2. Unlike the operator encoded by Γ_1 , that of Γ_2 is generally speaking not skew-symmetric with respect to its arguments. To extract its antisymmetric part, that is, the bi-vector encoded by Γ_2 , we use the formula $\frac{1}{2}(\Gamma_2(1, 2) - \Gamma_2(2, 1))$; admitting

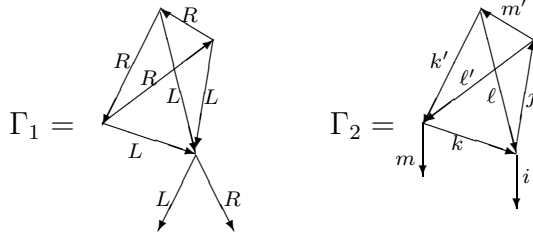


FIGURE 2. The Kontsevich tetrahedral graphs encode two bi-linear bi-differential operators on the product $C^\infty(N^n) \times C^\infty(N^n)$.

a slight abuse of notation in what follows, we shall still denote by the Γ_2 the skew-symmetrization of the second graph. To construct a class of flows on the space of bi-vectors, Kontsevich suggested to consider linear combinations, balanced by using the ratio $a : b$, of the graphs Γ_1 and Γ_2 . We recall from section 1.1 that every internal vertex of each graph is inhabited by a copy of a given Poisson bi-vector \mathcal{P} , so that the linear combination of two graphs encodes the bi-vector $\mathcal{Q}_{a:b}(\mathcal{P})$, quartic in \mathcal{P} and balanced using $a : b$. We now inspect at which ratio $(a : b)$ the bi-vector $\mathcal{P} + \varepsilon \mathcal{Q}_{a:b}(\mathcal{P}) + \bar{o}(\varepsilon)$ stays infinitesimally Poisson for $\varepsilon > 0$, that is (cf. Appendix A on p. 12),

$$[\mathcal{P} + \varepsilon \mathcal{Q}_{a:b}(\mathcal{P}) + \bar{o}(\varepsilon), \mathcal{P} + \varepsilon \mathcal{Q}_{a:b}(\mathcal{P}) + \bar{o}(\varepsilon)] = \bar{o}(\varepsilon). \quad (3)$$

Proposition 1 ([1]). The tetrahedral flow $\dot{\mathcal{P}} = \mathcal{Q}_{a:b}(\mathcal{P})$ preserves the property of $\mathcal{P} + \varepsilon \mathcal{Q}_{a:b}(\mathcal{P}) + \bar{o}(\varepsilon)$ to be infinitesimally Poisson for all Poisson bi-vectors \mathcal{P} on all affine real manifolds N^n only if the ratio is $a : b = 1 : 6$.

The proof amounts to producing at least one counterexample when any ratio other than $1 : 6$ violates equation (3) for a given Poisson bi-vector \mathcal{P} , see [1] for several such counterexamples.

In fact, more is known — this time, about the sufficiency of the condition $a : b = 1 : 6$.

Proposition 2 ($\mathbb{R}^3, \{\cdot, \cdot\}_{\mathcal{P}}$). The tetrahedral flow $\dot{\mathcal{P}} = \mathcal{Q}_{1:6}(\mathcal{P})$ does preserve the property of $\mathcal{P} + \varepsilon \mathcal{Q}_{a:b}(\mathcal{P}) + \bar{o}(\varepsilon)$ to be infinitesimally Poisson for all Poisson structures on \mathbb{R}^3 , which are described by using two arbitrary function in three Cartesian coordinates in the paper [4].

The proof is by direct calculation (e.g., assisted by software for symbolic transformations).¹

Expanding the LHS of equation (3), using the shifted-graded skew-symmetry of the Schouten bracket $[\cdot, \cdot]$, and taking into account that $[\mathcal{P}, \mathcal{P}] = 0$ if and only if \mathcal{P} is Poisson, we extract the (linear in deformation parameter ε) equation

$$[\mathcal{P}, \mathcal{Q}_{1:6}(\mathcal{P})] \doteq 0 \quad \text{mod } [\mathcal{P}, \mathcal{P}] = 0. \quad (1)$$

Let us examine the mechanism for the tri-vector $[\mathcal{P}, \mathcal{Q}_{1:6}(\mathcal{P})]$ in (1) to vanish by virtue of the Jacobi identity $\text{Jac}(\mathcal{P}) := [\mathcal{P}, \mathcal{P}] = 0$ for a given Poisson bi-vector \mathcal{P} .

¹Working in higher dimension, the construction from [4] does not provide an exhaustive description of Poisson structures on \mathbb{R}^n for $n \geq 4$. Nevertheless, we confirm that the claim remains true for the ratio $1 : 6$ for all Poisson structures of that class in dimensions 4 and 5.

Theorem 3. *There exists a polydifferential operator*

$$\diamond \in \text{PolyDiff} \left(\Gamma(\bigwedge^2 TN^n) \times \Gamma(\bigwedge^3 TN^n) \rightarrow \Gamma(\bigwedge^3 TN^n) \right) \quad (4)$$

which solves the factorization problem

$$[\![\mathcal{P}, \mathcal{Q}_{1:6}(\mathcal{P})]\!] = \diamond(\mathcal{P}, \text{Jac}(\mathcal{P})). \quad (5)$$

The polydifferential operator \diamond is realised using graphs in formula (6), see p. 8 below.

Corollary 4 (Main result). Whenever a bi-vector \mathcal{P} on an affine real manifold N^n is Poisson, the deformation $\mathcal{P} + \varepsilon \mathcal{Q}_{1:6}(\mathcal{P}) + \bar{o}(\varepsilon)$ using the Kontsevich tetrahedral flow is infinitesimally Poisson.

2. SOLUTION: FROM GRAPHS TO POLYDIFFERENTIAL OPERATORS

We now explain how the operator \diamond is found by using the method of undetermined coefficients in an expansion of all relevant graphical differential consequences of the Jacobi identity. By construction, the left-hand side of every such differential consequence is a sum of graphs with 5 internal vertices, of which 2 belong to the Jacobiator $\text{Jac}(\mathcal{P})$. (Another method for solution of factorization problem is outlined in Appendix D.)

Expanding the Leibniz rules in $[\![\mathcal{P}, \mathcal{Q}_{1:6}(\mathcal{P})]\!]$, we obtain the sum of 39 graphs with 5 internal vertices and 3 sinks; by construction, the Schouten bracket $[\![\mathcal{P}, \mathcal{Q}_{1:6}(\mathcal{P})]\!] \in \Gamma(\bigwedge^3 TN^n)$ is a tri-vector on the underlying manifold N^n , that is, it is a totally anti-symmetric tri-linear polyderivation $C^\infty(N^n) \times C^\infty(N^n) \times C^\infty(N^n) \rightarrow C^\infty(N^n)$. At the same time, we seek to recognize the tri-vector $[\![\mathcal{P}, \mathcal{Q}_{1:6}(\mathcal{P})]\!]$ as the result of application of the (poly)differential operator \diamond (see (5) in Theorem 3) to the Jacobiator $\text{Jac}(\mathcal{P})$ (see (2) on p. 3). We recall that for strictly positive differential order consequences of the Jacobi identity $\text{Jac}(\mathcal{P}) = 0$, the mechanism for operator \diamond to attain zero value at $\text{Jac}(\mathcal{P}) = 0$ is nontrivial. In fact, it refers to a (possibility of) splitting of every such consequence into the fragments which vanish independently from each other.

Lemma 5 ([2]). A tri-differential operator $C = \sum_{|I|, |J|, |K| \geq 0} c^{IJK} \partial_I \otimes \partial_J \otimes \partial_K$ with coefficients $c^{IJK} \in C^\infty(N^n)$ vanishes identically iff all its coefficients vanish: $c^{IJK} = 0$ for every triple (I, J, K) of multi-indices; here $\partial_L = \partial_1^{\alpha_1} \circ \cdots \circ \partial_n^{\alpha_n}$ for a multi-index $L = (\alpha_1, \dots, \alpha_n)$. Moreover, the fragments $C_{ijk} = \sum_{|I|=i, |J|=j, |K|=k} c^{IJK} \partial_I \otimes \partial_J \otimes \partial_K$ are zero for all differential orders (i, j, k) .

In practice, Lemma 5 states that for every arrow falling on the Jacobiator (for which, in turn, a triple of arguments is specified), the expansion of the Leibniz rule yields four fragments which vanish separately. Namely, there is the fragment such that the derivation acts on the content \mathcal{P} of the Jacobiator's two internal vertices, and there are three fragments such that the arrow falls on the first, second, or third argument of the Jacobiator. It is readily seen that the action of a derivative on an argument of the Jacobiator effectively amounts to an appropriate redefinition of its respective argument. Therefore, a restriction to the order $(1, 1, 1)$ is enough in the run-through over all the graphs which contain Jacobiator (2) and which stand on the three arguments f, g, h of the tri-vector $\diamond(\mathcal{P}, \text{Jac}(\mathcal{P}))$.

Remark 3. In all the above reasoning, the set $\{1, 2, 3\}$ of three arguments of the Jacobiator need not coincide with the set $\{f, g, h\}$ of the arguments of the tri-vector $\diamond(\mathcal{P}, \text{Jac}(\mathcal{P}))$. Of course, the two sets can intersect; this will provide a natural filtration for the components of solution (6). Namely, the number of elements in the intersection runs from three for the first term to zero in the second or third graph.

In fact, Remark 3 reveals a highly nontrivial role of the operator \diamond in (5). Indeed, some of the three internal vertices of its graphs can be the arguments of $\text{Jac}(\mathcal{P})$ whereas some of the other such vertices (if any) can be tails for the arrows falling on $\text{Jac}(\mathcal{P})$. In retrospect, the two subsets of such vertices of \diamond do not intersect; every vertex in the intersection, if it were nonempty, would produce a two-cycle, but there are no “eyes” in (6).

By ordering the Leibniz-rule graphs in the operator \diamond according to the number of Jacobiator’s arguments which simultaneously are the arguments of (totally skew-symmetric) tri-vector $[\mathcal{P}, \mathcal{Q}_{1:6}(\mathcal{P})] = \diamond(\mathcal{P}, \text{Jac}(\mathcal{P}))$, we count the number of variants in the run-through over all the admissible graphs. (With reference to Fig. 3 below, this is done in Appendix B, see p. 13.) In total, there are 1132 variants.

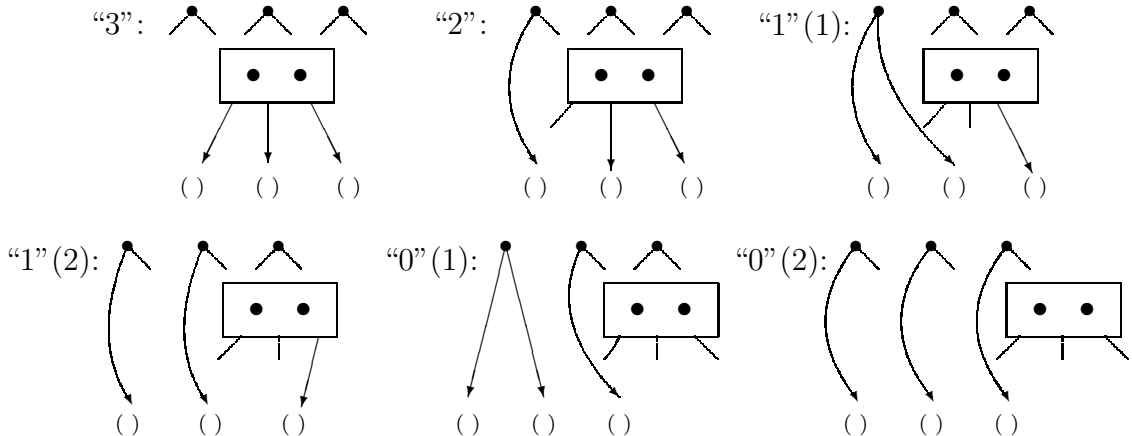


FIGURE 3. This is the list of all different types of differential consequences of the Jacobi identity which are linear in the Jacobiator and which are totally skew-symmetric with respect to the sinks. The list is ordered by the number of ground vertices on which the Jacobiator stands. The number of graphs for each type is deduced in Appendix B: namely, from top-left to bottom-right, there are 216, 432, 108, 288, 24, and 64 Leibniz-rule graphs. The total number of differential consequences is 1132.

We now split all these differential consequences of the Jacobi identity $\text{Jac}(\mathcal{P}) = 0$ by using Lemma 5 (with respect to the *total* differential order (i, j, k) for arguments of $\text{Jac}(\mathcal{P})$ if more than one arrow falls on it), ascribing an undetermined coefficient to every such separately vanishing fragment. That is, we do not restrict only to the differential order $(1, 1, 1)$ with respect to the arguments of $\text{Jac}(\mathcal{P})$ for every number of derivations acting on the Jacobiator; we agree that this way to introduce the undetermined coefficients is not minimal. However, we always restrict to the order $(1, 1, 1)$ with

respect to (f, g, h) . We thus have 28,202 unknowns introduced (counted with possible repetitions of graphs which they refer to). Now we expand all the Leibniz rules that run over the internal vertices in every Jacobiator; simultaneously, the object $\text{Jac}(\mathcal{P})$ is expanded using formula (2). As soon as we take into account the order $L \prec R$ and the antisymmetry of graphs under the reversion of that ordering at an internal vertex, the graphs that encode zero differential operators are eliminated. There remain 7,025 admissible graphs with 5 internal vertices and 3 sinks; the coefficient of every such graph is a linear combination of the undetermined coefficients of the splinters which the Leibniz-rule graphs (see Figure 3) produced from $\text{Jac}(\mathcal{P})$. In conclusion, we compose the inhomogeneous system of 7,025 equations with 28,202 unknowns.

Using software tools we solve this linear algebraic system; the duplications of graph labellings are conveniently eliminated by our request for the program to find a solution with a minimal number of nonzero components. Totally antisymmetric in tri-vector's arguments, the solution consists of 27 Leibniz-rule graphs, which are assimilated into the sum of 8 manifestly skew-symmetric terms as follows:

$$\begin{aligned}
 \diamond = & \text{Graph 1} + 3 \sum_{\tau \in S_2} (-)^{\tau} \text{Graph 2} + 3 \sum_{\circlearrowleft} \text{Graph 3} \\
 & + 3 \sum_{\circlearrowright} \left\{ \text{Graph 4} + \text{Graph 5} + \text{Graph 6} \right\} \\
 & + 3 \sum_{\sigma \in S_3} (-)^{\sigma} \left\{ \text{Graph 7} + \text{Graph 8} \right\} \quad (6)
 \end{aligned}$$

The formula above expands to 201 terms that collect to 39 graphs in the left-hand side $[\mathcal{P}, \mathcal{Q}_{1:6}(\mathcal{P})]$ of (5), as expected. To display the $L \prec R$ ordering at every internal vertex and to make possible the arithmetic and algebra of graphs, we use the notation which is explained in Appendix C below. By realizing the solution in both man- and machine readable format, we list the coefficients of all the 27 Leibniz-rule graphs within the found solution in Table 1 on p. 15.

3. DISCUSSION: PROPERTIES OF THE FOUND SOLUTION

Property 1. The relevant Leibniz-rule graphs, with respect to which the solution $\diamond(\mathcal{P}, \cdot)$ expands, do not contain tadpoles nor two-cycles (or “eyes”, see Fig. 1 on p. 4).

- None of the arrows that act back on the Jacobiator is issued from any of its arguments.

- In all the graphs the source vertices (if any), on which no arrows fall after all the Leibniz rules are expanded, belong to the Jacobiator (cf. (2) on p. 3).

Property 2. The found solution \diamond does contain the graphs in which two or three arrows fall on the Jacobiator.²

It has been explained in [6, 8] that the existence of two or more such arrows falling on the equation $[\![\mathcal{P}, \mathcal{P}]\!] = 0$ is an obstruction to an extension of the main claim,

$$[\![\mathcal{P}, \mathcal{Q}_{1:6}(\mathcal{P})]\!] \doteq 0 \pmod{[\![\mathcal{P}, \mathcal{P}]\!]} = 0, \quad (1)$$

to the infinite-dimensional geometry of jet spaces $J^\infty(\pi)$ for affine bundles over a manifold M^m or jet spaces $J^\infty(M^m \rightarrow N^n)$ of maps from M^m , and of variational Poisson brackets $\{ \cdot, \cdot \}_{\mathcal{P}}$ for functionals on such jet spaces (see [16, 5] and [7, 8]). Namely, it can then be that

$$[\![\mathcal{P}, \mathcal{Q}_{1:6}(\mathcal{P})]\!] \not\cong 0 \quad \text{though} \quad [\![\mathcal{P}, \mathcal{P}]\!] \cong 0. \quad (7)$$

We denote here by $[\![\cdot, \cdot]\!]$ the variational Schouten bracket; the variational bi-vector $\mathcal{Q}_{1:6}$ is constructed from the variational Poisson bi-vector \mathcal{P} by using techniques from the geometry of iterated variations of functionals (see [6, 7, 8]). An explicit counterexample of (7) is known from [1] for the variational Poisson structure of the Harry Dym partial differential equation.

The reason why the obstruction arises is that in the variational setting, the second and higher order variations of a trivial integral functional $\text{Jac}(\mathcal{P}) \cong 0$ in the horizontal cohomology can still be nonzero (although its first variation would of course vanish).³

Remark 4. Uniqueness is currently not claimed for the found solution $\diamond(\mathcal{P}, \cdot)$. The eight graphs in (6) represent a *linear* differential operator with respect to the Jacobiator $\text{Jac}(\mathcal{P})$. However, a quadratic nonlinearity with respect to the two-vertex argument $\text{Jac}(\mathcal{P})$ can be hidden in the five-vertex graphs in formula (6), so that it would in fact encode a polydifferential operator.

The scenarios to build the bi-linear, bi-differential terms in this operator \diamond are drawn in Figure 4 below. It remains for us to inspect whether there is or is not any quadratic part in the (poly)differential operator \diamond that solves factorisation problem (1).

Remark 5. The found shape of solution (6) is an expansion of the operator \diamond with respect to 27 Leibniz-rule graphs, now grouped in (6) into eight sums, each of them fully antisymmetric with respect to the three arguments of the tri-vector. All the coefficients of this expansion are integers; this property could manifest an intrinsic symmetry of

²For instance, the first term in \diamond is the tripod standing on $\text{Jac}(\mathcal{P})$.

³The same effect has been foreseen for a variational lift of deformation quantisation [13]: it has been argued in [8] why the associativity of noncommutative star-product $\star = \times + \hbar \{ \cdot, \cdot \}_{\mathcal{P}} + o(\hbar)$ can leak and it has been shown in [2] that if it actually does at $O(\hbar^k)$, the order k at which this leak of associativity can occur is high: $k \geq 4$.

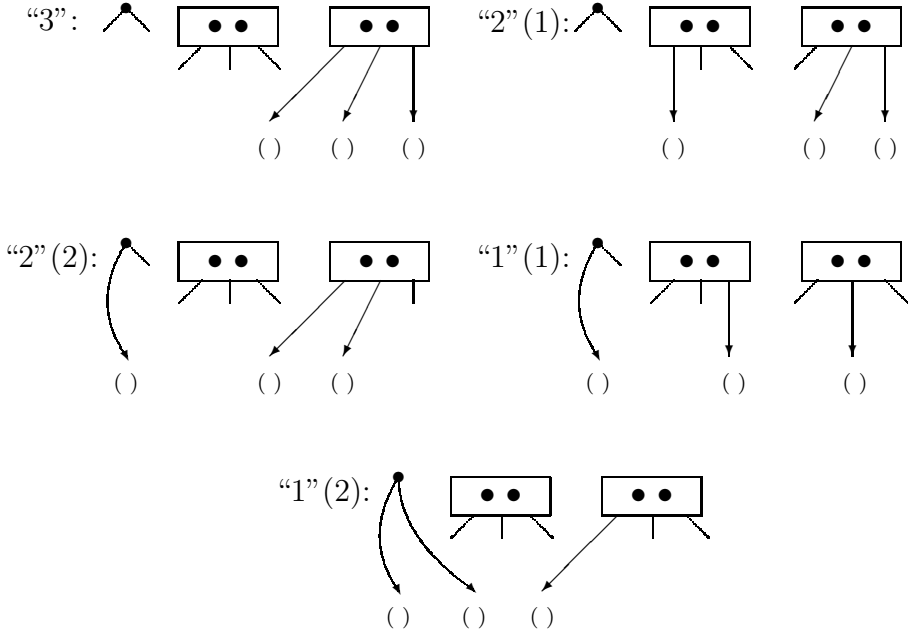


FIGURE 4. The Leibniz-graphs by using which a quadratic – with respect to the Jacobiator – part $\diamond(\mathcal{P}, \cdot, \cdot)$ of the factorizing operator could be sought for in (5); such quadratic part (if any) itself is necessarily totally skew-symmetric with respect to the three sinks ().

operator \diamond (for this solution in particular or for all solutions of (1)). The understanding of this symmetry mechanism would facilitate the future search of flows which, given by graphs over five or more vertices, preserve the space of Poisson bi-vectors on the affine manifold at hand.

4. CONCLUSION

4.1. For the factorisation $[\![\mathcal{P}, \mathcal{Q}_{1:6}(\mathcal{P})]\!] = \diamond(\mathcal{P}, \text{Jac}(\mathcal{P}))$ to guarantee that the equality $\partial_{\mathcal{P}}(\mathcal{Q}_{1:6}(\mathcal{P})) = 0$ holds if $\text{Jac}(\mathcal{P}) = 0$, its mechanism is nontrivial. Relying on Lemma 5 (see [2]), it tells us how the differential consequences of Jacobi identity are split into separately vanishing expressions. This mechanism works not only in the construction of flows that satisfy (1) but also in the associativity,

$$\text{Assoc}_{\mathcal{P}}(f, g, h) := (f \star g) \star h - f \star (g \star h) \stackrel{.}{=} 0 \pmod{[\![\mathcal{P}, \mathcal{P}]\!]} = 0,$$

of the non-commutative unital star-product $\star = \times + \hbar \{ \cdot, \cdot \}_{\mathcal{P}} + o(\hbar)$. The formula for \star -products was given in [13], establishing the deformation quantisation $\times \mapsto \star$ of the usual product \times in the algebra $C^{\infty}(N^n) \ni f, g, h$ on a finite-dimentional affine Poisson manifold (N^n, \mathcal{P}) , see also [2, 8]. In fact, the construction of graph complex and the pictorial language of graphs [12, 13] that encode polydifferential operators is common to all these deformation procedures.

Open problem 1. Consider the Kontsevich star-product $\star = \times + \hbar \{ \cdot, \cdot \}_{\mathcal{P}} + o(\hbar)$ in the algebra $C^\infty(N^n)[[\hbar]]$ on a finite-dimensional affine Poisson manifold (N^n, \mathcal{P}) . Given by the tetrahedra Γ_1 and Γ_2 (see Fig. 2 on p. 5), the infinitesimal deformation $\mathcal{P} \mapsto \mathcal{P} + \varepsilon \mathcal{Q}_{1:6}(\mathcal{P}) + o(\varepsilon)$ induces the infinitesimal deformation $\star \mapsto \star + \hbar \varepsilon [[\mathcal{Q}_{1:6}(\mathcal{P}), \cdot], \cdot]] + o(\varepsilon)$ of the star-product. What are the properties of this infinitesimally deformed $\star(\varepsilon)$ -product? In particular, is the condition that $\mathcal{Q}_{1:6}(\mathcal{P})$ be $\partial_{\mathcal{P}}$ -trivial necessary for the $\star(\varepsilon)$ -product to be gauge-equivalent to the unperturbed \star -product at $\varepsilon = 0$?

4.2. The Kontsevich tetrahedral flow $\dot{\mathcal{P}} = \mathcal{Q}_{1:6}(\mathcal{P})$ is a universal procedure to deform a given Poisson bi-vector \mathcal{P} on any finite-dimensional affine real manifold N^n (i. e., not necessarily topologically trivial). The infinitesimal deformation $\mathcal{P} \mapsto \mathcal{P} + \varepsilon \mathcal{Q}_{1:6}(\mathcal{P}) + o(\varepsilon)$ can be completed to the construction of Poisson bi-vector $\mathcal{P}(\varepsilon)$ such that $\mathcal{P}(\varepsilon = 0) = \mathcal{P}$ and $\frac{d}{d\varepsilon}|_{\varepsilon=0} \mathcal{P}(\varepsilon) = \mathcal{Q}_{1:6}(\mathcal{P})$ if the third Poisson cohomology group $H_{\mathcal{P}}^3(N^n)$ with respect to the Poisson differential $\partial_{\mathcal{P}} = [\mathcal{P}, \cdot]$ vanishes for the manifold N^n (see Appendix A below). In the symplectic case, i. e. for n even and bracket $\{ \cdot, \cdot \}_{\mathcal{P}}$ nondegenerate, the Poisson complex is known to be isomorphic to the de Rham complex for N^n (see [14]). We are not yet aware of any way to constrain the Poisson cohomology groups $H_{\mathcal{P}}^k(N^n)$ for *degenerate* Poisson brackets $\{ \cdot, \cdot \}_{\mathcal{P}}$ on real manifolds N^n of not necessarily even dimension $n < \infty$.

4.3. The second de Rham cohomology group $H_{\text{dR}}^2(N^n)$ of the manifold N^n , if nonzero, provides room for the $\partial_{\mathcal{P}}$ -nontrivial deformations of \mathcal{P} using $\mathcal{Q}_{1:6}(\mathcal{P})$ such that $\mathcal{Q}_{1:6}(\mathcal{P}) \neq [[\mathcal{P}, \mathcal{X}]]$ for all globally defined 1-vectors \mathcal{X} on N^n . In particular, this implies that there are no $\partial_{\mathcal{P}}$ -nontrivial tetrahedral graph flows on even-dimensional star-shaped domains equipped with nondegenerate Poisson brackets.

A possibility for the right-hand side $\mathcal{Q}_{1:6}(\mathcal{P})$ of the tetrahedral flow to be $\partial_{\mathcal{P}}$ -trivial is thus a global, topological effect; it cannot always be seen within a single chart in N^n . Moreover, it is not universal with respect to the calculus of graphs.

Claim 6. *In contrast with Theorem 3, there is no $\partial_{\mathcal{P}}$ -triviality mechanism which would be expressed for the tetrahedral flow $\dot{\mathcal{P}} = \mathcal{Q}_{1:6}(\mathcal{P})$ in terms of the Kontsevich graphs (see §1.1 and [12, 13]) and hence, which would be universal with respect to all Poisson structures \mathcal{P} on all finite-dimensional affine manifolds N^n .*

Proof. Indeed, consider the $\partial_{\mathcal{P}}$ -coboundary equation,

$$\Gamma_1(f, g) + \frac{6}{2}(\Gamma_2(f, g) - \Gamma_2(g, f)) = [[\begin{array}{c} \nearrow \\ \searrow \end{array}, \mathcal{X}]](f, g),$$

where the graphs Γ_1 and Γ_2 , inhabited by a copy of the Poisson bi-vector \mathcal{P} in every internal vertex, are shown in Fig. 2 on p. 5. Because there are four copies of \mathcal{P} in each tetrahedron and the Λ -graph in $\partial_{\mathcal{P}} = [[\mathcal{P}, \cdot]]$ contains one copy of the bi-vector \mathcal{P} , the number of internal vertices in the 1-vector \mathcal{X} must be equal to 3. The only such Kontsevich graph without tadpoles is

$$\mathcal{X} = \text{const} \cdot \begin{array}{c} \nearrow \\ \searrow \end{array} .$$

Now it is readily seen that the Schouten bracket of \mathcal{X} with the Poisson bi-vector \mathcal{P} does contain a source vertex (to which no arrows arrive). But there is no such vertex in either of the tetrahedra within the bi-vector $\mathcal{Q}_{1:6}(\mathcal{P})$ in the left-hand side of the $\partial_{\mathcal{P}}$ -cocycle equation $\mathcal{Q}_{1:6}(\mathcal{P}) = \partial_{\mathcal{P}}(\mathcal{X})$. This shows that there is no universal solution $\mathcal{X}(\mathcal{P})$ expressed for all \mathcal{P} in terms of graphs. \square

Remark 6. The same reasoning works for all the Kontsevich graph flows such that none of the graphs besides the bi-vector \mathcal{P} itself contains a source vertex (that is, neither the flow nor the 1-vector \mathcal{X}).

Open problem 2. The formalism developed in [12] suggests that there are, most likely, infinitely many Kontsevich graph flows on the spaces of Poisson bi-vectors on finite-dimensional affine Poisson manifolds. Forming an example $\mathcal{Q}_{1:6}(\mathcal{P})$ of such a cocycle in the graph complex, the tetrahedra Γ_1 and Γ_2 in Fig. 2 are built over four internal vertices. What is or are the next – with respect to the ordering of natural numbers – Kontsevich graph cocycle(s) built over five or more internal vertices?

4.4. The tetrahedral flow $\dot{\mathcal{P}} = \mathcal{Q}_{1:6}(\mathcal{P})$ preserves the space $\{\mathcal{P} \in \Gamma(\bigwedge^2 TN^n) \mid [\![\mathcal{P}, \mathcal{P}]\!] = 0\}$ of Poisson bi-vectors; this is guaranteed by Theorem 3 that asserts $\partial_{\mathcal{P}}(\mathcal{Q}_{1:6}) \dot{=} 0$ within the (graded-)commutative geometry of finite-dimensional affine real manifolds N^n .

Open problem 3. Does the proven property,

$$[\![\mathcal{P}, \mathcal{Q}_{1:6}(\mathcal{P})]\!] \dot{=} 0 \mod [\![\mathcal{P}, \mathcal{P}]\!] = 0, \quad (1)$$

generalize to the formal noncommutative symplectic supergeometry [9], to the calculus of multivectors performed by using their necklace brackets (see [7] and references therein), and to Poisson structures on the commutative non-associative unital algebras of cyclic words (e.g., see [17])?

Acknowledgements. A. K. thanks M. Kontsevich for posing the problem; the authors are grateful to P. Vanhaecke for stimulating discussions.

This research was supported in part by JBI RUG project 106552 (Groningen). A. B. and R. B. thank the organizers of the 8th international workshop GADEIS VIII on Group Analysis of Differential Equations and Integrable Systems (12–16 June 2016, Larnaca, Cyprus) for partial financial support and warm hospitality. A. B. and R. B. are also grateful to the Graduate School of Science (Faculty of Mathematics and Natural Sciences, University of Groningen) for financial support. We thank the Center for Information Technology of the University of Groningen for providing access to the Peregrine high performance computing cluster.

APPENDIX A. THE POISSON COHOMOLOGY

Let us recall several necessary facts from the deformation theory; this material is standard [3]. Denote by ξ_i the parity-odd canonical conjugate of the variable x^i for every $i = 1, \dots, n$ (see [7] for discussion about the reverse parity symplectic duals). Every bi-vector is then realised in terms of the local coordinates x^i and ξ_i on $\Pi T^* N^n$ by using

$\mathcal{P} = \frac{1}{2} \langle \xi_i \mathcal{P}^{ij}(\mathbf{x}) \xi_j \rangle$. We denote by $[\![\cdot, \cdot]\!]$ the Schouten bracket, i.e., the parity-odd Poisson bracket which is locally determined on $\Pi T^* \mathbb{R}^n$ by the canonical symplectic structure $d\mathbf{x} \wedge d\boldsymbol{\xi}$ (see [6] for details). Currently, our working formula is⁴

$$[\![\mathcal{P}, \mathcal{Q}]\!] = (\mathcal{P}) \overleftarrow{\frac{\partial}{\partial x^i}} \cdot \overrightarrow{\frac{\partial}{\partial \xi_i}}(\mathcal{Q}) - (\mathcal{P}) \overleftarrow{\frac{\partial}{\partial \xi_i}} \cdot \overrightarrow{\frac{\partial}{\partial x^i}}(\mathcal{Q}).$$

To be Poisson, a bi-vector \mathcal{P} must satisfy the master-equation $[\![\mathcal{P}, \mathcal{P}]\!] = 0$, of which formula (2) is the component expansion with respect to the indices (i, j, k) in the trivector $[\![\mathcal{P}, \mathcal{P}]\!](\mathbf{x}, \boldsymbol{\xi})$.

Under an infinitesimal deformation $\mathcal{P}(\varepsilon) = \mathcal{P} + \varepsilon \mathcal{Q} + \bar{o}(\varepsilon)$ of the bi-vector \mathcal{P} satisfying $[\![\mathcal{P}, \mathcal{P}]\!] = 0$, the bi-vector $\mathcal{P}(\varepsilon)$ remains Poisson only if $[\![\mathcal{P}(\varepsilon), \mathcal{P}(\varepsilon)]!] = \bar{o}(\varepsilon)$, whence $[\![\mathcal{P}, \mathcal{Q}]\!] = 0$.

Remark 7. For a Poisson bi-vector \mathcal{P} , the operator $\partial_{\mathcal{P}} = [\![\mathcal{P}, \cdot]\!]$ is readily seen to be a differential: by virtue of the Jacobi identity for the Schouten bracket $[\![\cdot, \cdot]\!]$ we have that $\partial_{\mathcal{P}}^2 = 0$. Therefore, the leading order terms \mathcal{Q} in the deformations $\mathcal{P}(\varepsilon) = \mathcal{P} + \varepsilon \mathcal{Q} + \bar{o}(\varepsilon)$ can be trivial in the second $\partial_{\mathcal{P}}$ -cohomology, meaning that $\mathcal{Q} = [\![\mathcal{P}, \mathcal{X}]\!]$ for some one-vector \mathcal{X} (whence $[\![\mathcal{P}, [\![\mathcal{P}, \mathcal{X}]\!]] \equiv 0$). Alternatively, for the $\partial_{\mathcal{P}}$ -cocycles \mathcal{Q} which are not $\partial_{\mathcal{P}}$ -coboundaries, the flows $\mathcal{P}(\varepsilon)$ stay infinitesimally Poisson but leave the $\partial_{\mathcal{P}}$ -cohomology class of the Poisson bi-vector \mathcal{P} at $\varepsilon = 0$.

For consistency, let us recall that generally speaking, not every infinitesimal deformation $\mathcal{P} \mapsto \mathcal{P} + \varepsilon \mathcal{Q} + \bar{o}(\varepsilon)$ of a Poisson bi-vector \mathcal{P} can be completed to a Poisson deformation $\mathcal{P} \mapsto \mathcal{P} + \mathcal{Q}(\varepsilon)$ at all orders in ε . The obstructions are contained in the third $\partial_{\mathcal{P}}$ -cohomology group $H_{\mathcal{P}}^3 = \{T \in \Gamma(\bigwedge^3 TN) \mid \partial_{\mathcal{P}}(T) = 0\} / \{T = \partial_{\mathcal{P}}(R), R \in \Gamma(\bigwedge^2 TN)\}$. Indeed, cast the master-equation $[\![\mathcal{P} + \mathcal{Q}(\varepsilon), \mathcal{P} + \mathcal{Q}(\varepsilon)]!] = 0$ for the Poisson deformation to the coboundary statement $[\![\mathcal{Q}(\varepsilon), \mathcal{Q}(\varepsilon)]!] = \partial_{\mathcal{P}}(-\mathcal{P} - 2\mathcal{Q}(\varepsilon))$ within $O^*(\varepsilon^2)$, whence $\partial_{\mathcal{P}}([\![\mathcal{Q}(\varepsilon), \mathcal{Q}(\varepsilon)]!]) \equiv 0$ by $\partial_{\mathcal{P}}^2 = 0$. Therefore, the vanishing of the third $\partial_{\mathcal{P}}$ -cohomology group guarantees the existence of a power series solution $\mathcal{Q}(\varepsilon)$ to the cocycle-coboundary equation $[\![\mathcal{Q}(\varepsilon), \mathcal{Q}(\varepsilon)]!] = -2\partial_{\mathcal{P}}(\mathcal{Q}(\varepsilon))$: known to be a cocycle, the left-hand side has been proven to be a coboundary as well.

Remark 8. Nowhere above should one expect that the leading deformation term \mathcal{Q} in $\mathcal{P}(\varepsilon) = \mathcal{P} + \varepsilon \mathcal{Q} + \bar{o}(\varepsilon)$ itself would be a Poisson bi-vector. This may happen for \mathcal{Q} only incidentally.

APPENDIX B. THE COUNT OF LEIBNIZ-RULE GRAPHS IN FIG. 3

We count all possible differential consequences of the Jacobi identity, that is, we consider the differential operators acting on the Jacobiator. We do this by constructing all possible graphs that encode trivector-valued differential consequences (see Lemma 5 on p. 6). The graphs that encode such differential consequences have 3 ground vertices. The Schouten bracket $[\![\mathcal{P}, \mathcal{Q}_{1:6}(\mathcal{P})]\!]$ consists of graphs with 5 internal vertices. Since

⁴In the set-up of infinite jet spaces $J^\infty(\pi)$ (see [16] and [6, 7, 8]) the four partial derivatives in the formula for $[\![\cdot, \cdot]\!]$ become the variational derivatives with respect to the same variables, which now parametrise the fibres in the Whitney sum $\pi \times_{M^m} \Pi \widehat{\pi}$ of (super-)bundles over the m -dimensional base M^m .

two of these internal vertices are accounted for the Jacobi identity, there remain 3 spare internal vertices.

First, let the Jacobiator stand, with all its three edges, on the 3 ground vertices. The only freedom that remains is how the 3 free internal vertices act on each other and on the Jacobiator. With its first edge, every free internal vertex can act on itself, on its 2 neighbouring free vertices, or on the Jacobiator; there are 4 possible targets. No second edge can meet the first edge at the same target (as this would yield no contribution due to the anti-symmetry, which is explained in Remark 2). Hence there are only 3 possible targets for this second edge. Finally, again due to anti-symmetry, every possibility is constructed exactly twice this way. Swapping the targets of the first and second edge only contributes to the sign of the graph. The total number of this type of differential consequence is therefore $(\frac{4 \cdot 3}{2})^3 = 216$ graphs. This type of graph is drawn first from the top-left in Figure 3.

Now let the Jacobiator stand on only 2 of the ground vertices. The remaining edge of the Jacobiator has only 3 possible targets, as the third edge cannot fall back onto the Jacobiator itself. One of the free internal vertices acts with an edge on the remaining ground vertex. The other edge has 4 candidates as its target, namely the vertex itself, the neighbouring 2 free internal vertices, and the Jacobiator. The 2 internal vertices not falling on a ground vertex have each $\frac{4 \cdot 3}{2}$ possible targets. The total number of graphs is therefore equal to $3 \cdot 4 \cdot (\frac{4 \cdot 3}{2})^2 = 432$. This type of graph is the second from the top-left in Figure 3.

Next, let the Jacobiator stand on only 1 ground vertex. We distinguish between two cases: namely, the case where 1 free internal vertex stands on both the remaining ground vertices and the case where two different internal vertices act by one edge each on the remaining two ground vertices. These are the third and fourth graphs from the top-left in Figure 3, respectively.

- In the first case, the remaining 2 internal vertices each have $\frac{4 \cdot 3}{2}$ possible targets. The Jacobiator must act with its two remaining free edges on two different targets out of the 3 available, yielding 3 possibilities. The number of graphs in the first case is $3 \cdot (\frac{4 \cdot 3}{2})^2 = 108$.
- For the second case, two internal vertices can each act on themselves, on the neighbouring 2 internal vertices, or on the Jacobiator. With two of its edges, the Jacobiator can act in 3 different ways on the 3 internal vertices. The third internal vertex has $\frac{4 \cdot 3}{2}$ possible targets. This brings the total number of graphs for the second case to $4 \cdot 4 \cdot \frac{4 \cdot 3}{2} \cdot 3 = 288$.

The last case to consider is where the Jacobiator does not act on any of the ground vertices. Again, since the outgoing edges of the Jacobiator must have different targets, it is clear that the Jacobiator acts in a unique way on all 3 internal vertices. We now distinguish two cases: namely, the case where 1 free internal vertex stands on 2 ground vertices, 1 free internal vertex acts on 1 ground vertex, and 1 free internal vertex falling on no ground vertex, and the second case where each internal vertex acts with one edge on one ground vertex. These two cases are represented by the last 2 graphs in Figure 3, respectively.

- In the first case, there is a free internal vertex with one free edge, which has 4

possible targets. The remaining free internal vertex with two free edges has $\frac{4 \cdot 3}{2}$ possible targets. The total number of graphs for this case is $4 \cdot \frac{4 \cdot 3}{2} = 24$.

- In the second case, each internal vertex can act on itself, on its 2 neighbouring internal vertices, and on the Jacobiator. This results in a total of $4^3 = 64$ graphs.

Summarizing, the total number of all trivector-valued Leibniz-rule graphs, linear in the Jacobiator and containing five internal vertices, is 1132.

APPENDIX C. ENCODING OF THE SOLUTION

Let Γ be a labelled Kontsevich graph with n internal and m external vertices. We assume the ground vertices of Γ are labelled $[0, \dots, m-1]$ and the internal vertices are labelled $[m, \dots, m+n-1]$. We define the *encoding* of Γ to be the *prefix* (n, m) , followed by a list of *targets*. The list of targets consists of ordered pairs where the k th pair ($k \geq 0$) contains the two targets of the internal vertex number $m+k$.

Consisting of 8 skew-symmetric terms, the solution (see (6) on p. 8) is encoded in Table 1: the sought-for values of coefficients are written after the encoding of the respective 27 Leibniz-rule graphs.⁵ Here the sums over permutations of the ground vertices

1. 3 5 4 6 5 6 3 6 0 1 6 2	1	15. 3 5 0 5 2 3 4 6 1 3 6 4	-3
2. 3 5 5 6 2 3 4 6 0 1 6 4	3	16. 3 5 0 5 3 5 2 6 1 3 6 4	-3
3. 3 5 5 6 3 5 2 6 0 1 6 4	3	17. 3 5 2 5 3 5 0 6 1 3 6 4	3
4. 3 5 1 4 5 6 3 6 0 2 6 3	-3	18. 3 5 0 5 3 5 1 6 2 3 6 4	3
5. 3 5 4 5 1 6 4 6 0 2 6 3	3	19. 3 5 1 5 3 5 0 6 2 3 6 4	-3
6. 3 5 1 2 3 5 3 6 0 3 6 4	-3	20. 3 5 4 6 0 1 3 4 2 4 6 5	3
7. 3 5 1 4 2 5 3 6 0 3 6 4	3	21. 3 5 4 6 0 5 1 3 2 4 6 5	3
8. 3 5 1 5 2 3 4 6 0 3 6 4	3	22. 3 5 4 6 1 5 0 3 2 4 6 5	-3
9. 3 5 1 5 3 5 2 6 0 3 6 4	3	23. 3 5 0 1 2 3 3 4 3 4 6 5	3
10. 3 5 2 5 3 5 1 6 0 3 6 4	-3	24. 3 5 0 2 1 3 3 4 3 4 6 5	-3
11. 3 5 0 4 5 6 3 6 1 2 6 3	3	25. 3 5 0 4 1 2 3 4 3 4 6 5	3
12. 3 5 4 5 0 6 4 6 1 2 6 3	-3	26. 3 5 0 4 1 5 2 3 3 4 6 5	3
13. 3 5 0 2 3 5 3 6 1 3 6 4	3	27. 3 5 0 4 2 5 1 3 3 4 6 5	-3
14. 3 5 0 4 2 5 3 6 1 3 6 4	-3		

TABLE 1. Machine-readable encoding of solution (6) on p. 8.

are expanded (thus making the 27 Leibniz-rule graphs out of the 8 skew-symmetric groups). In every entry of Table 1, the sum of three graphs in (2) is represented by its first term. For all the in-coming arrows, the vertex 6 is the placeholder for the Jacobiator (again, see (2) on p. 3); in earnest, the Jacobiator contains the internal vertices 6 and 7. This convention is helpful: for every set of derivations acting on the Jacobiator with internal vertices 6 and 7, only the first term is listed, namely the one where each edge lands on 6.

Example 1. The first entry of Table 1 encodes a three-cycle over internal vertices 3, 4, 5. Issued from each of these three, the other edge lands on the vertex 6, which is

⁵Automatically generated, the entries in Table 1 contain no misprints.

the placeholder for the Jacobiator. This entry corresponds to the first term in (6) on p. 8.

APPENDIX D. PERTURBATION METHOD

In section 2 above, the run-through method gave all the terms at once in the operator \diamond that establishes the factorization $[\![\mathcal{P}, \mathcal{Q}_{1:6}]\!] = \diamond(\mathcal{P}, \text{Jac}(\mathcal{P}))$. At the same time, there is another method to find \diamond ; the operator \diamond is then constructed gradually, term after term in (6), by starting with a zero initial approximation for \diamond . This is the perturbation scheme which we now outline.

In fact, the perturbation method was tried first, revealing the typical graph patterns and their topological complexity. From Proposition 2 we already know that $[\![\mathcal{P}, \mathcal{Q}_{1:6}]\!] = 0$ for Poisson brackets on \mathbb{R}^3 . The difficulty is that because the condition $[\![\mathcal{P}, \mathcal{Q}_{1:6}]\!] = 0$ and the Jacobi identity $[\![\mathcal{P}, \mathcal{P}]\!] = 0$ are valid, it is impossible to factorize one through the other; both are invisible. So, we first make both expressions visible by perturbing the Poisson bi-vector $\mathcal{P} \mapsto \mathcal{P}_\epsilon = \mathcal{P} + \epsilon \Delta$ in such a way that the tri-vector $[\![\mathcal{P}, \mathcal{Q}_{1:6}(\mathcal{P}_\epsilon)]\!]$ and the Jacobiator $[\![\mathcal{P}_\epsilon, \mathcal{P}_\epsilon]\!]$ stop vanishing identically:

$$[\![\mathcal{P}, \mathcal{Q}_{1:6}(\mathcal{P}_\epsilon)]\!] \neq 0 \quad \text{and} \quad [\![\mathcal{P}_\epsilon, \mathcal{P}_\epsilon]\!] \neq 0.$$

To begin with, put $\diamond := 0$. Now consider the description [4] of Poisson brackets on \mathbb{R}^3 by using the pre-factor $f(x^1, x^2, x^3)$ and arbitrary function $g(x^1, x^2, x^3)$ in the formula

$$\{a, b\}_{\mathcal{P}} = f \cdot \left| \frac{\mathcal{D}(g, a, b)}{\mathcal{D}(x^1, x^2, x^3)} \right|;$$

it is helpful to start with some very degenerate dependencies of f and g of their arguments. The next step is to perturb the coefficients of the Poisson bracket $\{\cdot, \cdot\}_{\mathcal{P}}$ at hand; in a similar way, one starts with degenerate dependency of the perturbation Δ . The idea is to take perturbations which destroy the validity of Jacobi identity for \mathcal{P}_ϵ in the linear approximation in the deformation parameter ϵ . It is readily seen that the expansion of (5) in ϵ yields the equality

$$[\![\mathcal{P}, \mathcal{Q}_{1:6}]\!(\epsilon) = (\diamond + \bar{o}(1)) ([\![\mathcal{P}_\epsilon, \mathcal{P}_\epsilon]\!]) = 2\epsilon \cdot (\diamond + \bar{o}(1)) ([\![\mathcal{P}, \Delta]\!]) + (0 + \bar{o}(1)) ([\![\mathcal{P}, \mathcal{P}]\!]) + \bar{o}(\epsilon).$$

Knowing the left-hand side at first order in ϵ and taking into account that $[\![\mathcal{P}, \mathcal{P}]\!] \equiv 0$ for the Poisson bi-vector \mathcal{P} which we perturb by Δ , we reconstruct the operator \diamond that now acts on the known tri-vector $2[\![\mathcal{P}, \Delta]\!]$. In this sense, the Jacobiator $[\![\mathcal{P}, \mathcal{P}]\!]$ shows up through the term $[\![\mathcal{P}, \Delta]\!]$.

For each pair (\mathcal{P}, Δ) , the above balance at ϵ^1 contains sums over indexes that mark the derivatives falling on the Jacobiator. By taking those formulae, we guess the candidates for graphs that form the next, yet unknown, part of the operator \diamond . Specifically, we inspect which differential operator(s), acting on the Jacobi identity, become visible and we list the graphs that provide such differential operators via the Leibniz rule(s). For a while we keep every such candidate with an undetermined coefficient. By repeating the iteration, now for a different Poisson bi-vector \mathcal{P} or its new, less degenerate perturbation Δ , we obtain linear constraints for the already introduced undetermined coefficients. Simultaneously, we continue listing the new candidates and introducing new coefficients for them.

Remark 9. By translating formulae into graphs, we convert the dimension-dependent expressions into the dimension-independent operators which are encoded by the graphs. An obvious drawback of the method which is outlined here is that, presumably, some parts of the operator \diamond could always stay invisible for all Poisson structures over \mathbb{R}^3 if they show up only in the higher dimensions. Secondly, the number of variants to consider and in practice, the number of irrelevant terms, each having its own undetermined coefficient, grows exponentially at the initial stage of the reasoning.

By following the loops of iterations of this algorithm, we managed to find two non-zero coefficients and five zero coefficients in solution (6). Namely, we identified the coefficient ± 1 for the tripod, which is the first term in (6), and we also recognized the coefficient ± 3 of the sum of ‘elephant’ graphs, which is the second to last term in (6).

Remark 10. Because of the known skew-symmetry of the tri-vector $[\![\mathcal{P}, \mathcal{Q}_{1:6}]\!]$ with respect to its arguments f, g, h , finding one term in a sum within formula (6) for \diamond means that the entire such sum is reconstructed. Indeed, one then takes the sum over a subgroup of S_3 acting on f, g, h , depending on the actual skew-symmetry of the term which has been found.

For instance, the first term in (6), itself making a sum running over $\{\text{id}\} \prec S_3$, is obviously totally antisymmetric with respect to its arguments. On the other hand, the graph which we found by using the perturbation method (see the last graph in the second line of formula (6) on p. 8) is skew-symmetric with respect to its second and third arguments but it is not yet totally skew-symmetric with respect to the full set of its arguments. This shows that it suffices to take the sum over the group $\circlearrowleft = A_3 \prec S_3$ of cyclic permutations of f, g, h , thus reconstructing the sixth term in solution (6).

REFERENCES

- [1] *Bouisaghouane A., Kiselev A. V. (2016) Do the Kontsevich tetrahedral flows preserve or destroy the space of Poisson bi-vectors?* *Preprint IHÉS/M/16/12* (Bures-sur-Yvette, France), 12 pp.
- [2] *Buring R., Kiselev A. V. (2017) On the Kontsevich \star -product associativity mechanism,* *PEPAN Letters* **14**:2 (accepted), 4 p. (*Preprint arXiv:1602.09036 [q-alg]*)
- [3] *Gerstenhaber M. (1964) On the deformation of rings and algebras,* *Ann. Math.* **79**, 59–103.
- [4] *Grabowski J., Marmo G., Perelomov A. M. (1993) Poisson structures: towards a classification,* *Mod. Phys. Lett.* **A8**:18, 1719–1733.
- [5] *Kiselev A. V. (2012) The twelve lectures in the (non)commutative geometry of differential equations,* *Preprint IHÉS/M/12/13* (Bures-sur-Yvette, France), 140 pp.
- [6] *Kiselev A. V. (2013) The geometry of variations in Batalin–Vilkovisky formalism,* *J. Phys.: Conf. Ser.* **474**, Paper 012024, 1–51. (*Preprint 1312.1262 [math-ph]*)
- [7] *Kiselev A. V. (2015) The calculus of multivectors on noncommutative jet spaces.* *Preprint IHÉS/M/14/39* (Bures-sur-Yvette, France), *arXiv:1210.0726* (v3) [math.DG], 41 p.
- [8] *Kiselev A. V. (2015) Deformation approach to quantisation of field models,* *Preprint IHÉS/M/15/13* (Bures-sur-Yvette, France), 37 p.

- [9] Kontsevich M. (1993) Formal (non)commutative symplectic geometry, The Gel'fand Mathematical Seminars, 1990-1992 (L. Corwin, I. Gelfand, J. Lepowsky, eds), Birkhäuser, Boston MA, 173–187.
- [10] Kontsevich M. (1994) Feynman diagrams and low-dimensional topology. First Europ. Congr. of Math. **2** (Paris, 1992), Progr. Math. **120**, Birkhäuser, Basel, 97–121.
- [11] Kontsevich M. (1995) Homological algebra of mirror symmetry. Proc. Intern. Congr. Math. **1** (Zürich, 1994), Birkhäuser, Basel, 120–139.
- [12] Kontsevich M. (1997) Formality conjecture. Deformation theory and symplectic geometry (Ascona 1996, D. Sternheimer, J. Rawnsley and S. Gutt, eds), Math. Phys. Stud. **20**, Kluwer Acad. Publ., Dordrecht, 139–156.
- [13] Kontsevich M. (2003) Deformation quantization of Poisson manifolds, *Lett. Math. Phys.* **66**:3, 157–216. (Preprint [q-alg/9709040](#))
- [14] Laurent–Gengoux C., Pichereau A., Vanhaecke P. (2013) Poisson structures. Grundlehren der mathematischen Wissenschaften **347**, Springer–Verlag, Berlin.
- [15] Merkulov S. A. (2010) Exotic automorphisms of the Schouten algebra of polyvector fields. Preprint [arXiv:0809.2385](#) (v6) [q-alg], 37 p.
- [16] Olver P. J. (1993) Applications of Lie groups to differential equations, Grad. Texts in Math. **107** (2nd ed.), Springer–Verlag, NY.
- [17] Olver P. J., Sokolov V. V. (1998) Integrable evolution equations on associative algebras, *Comm. Math. Phys.* **193**:2, 245–268;
Olver P. J., Sokolov V. V. (1998) Non-abelian integrable systems of the derivative nonlinear Schrödinger type, *Inverse Prob.* **14**:6, L5–L8.
- [18] Vanhaecke P. (1996) Integrable systems in the realm of algebraic geometry, Lect. Notes Math. **1638**, Springer–Verlag, Berlin.